Supplemental Document

Biomedical Optics EXPRESS

Versatile, do-it-yourself, low-cost spinning disk confocal microscope: supplement

AARON R. HALPERN,[1,4] MIN YEN LEE,[1] MARCO D. HOWARD,[1] MARCUS A. WOODWORTH,[1] PHILIP R. NICOVICH,[2] AND JOSHUA C. VAUGHAN[1,3,5]

[1] *University of Washington, Department of Chemistry, Seattle, WA 98195, USA*
[2] *Allen Institute for Brain Science, Seattle, WA 98195, USA*
[3] *University of Washington, Department of Physiology and Biophysics, Seattle, WA 98195, USA*
[4] *aaron.halpern@gmail.com*
[5] *jcv2@uw.edu*

Supplement DOI: https://doi.org/10.6084/m9.figshare.18711923

Parent Article DOI: https://doi.org/10.1364/BOE.442087

Versatile, do-it-yourself, low-cost spinning disk confocal microscope: Supplemental Document

Table S1. Component list for DIY spinning disk confocal microscope. The components below are meant to be incorporated onto an existing microscope system including chassis, camera, and lasers, which depending on configuration may cost from $100,000-$200,000 (see also Supplemental Note 3).

Component Name	Vendor	Catalog #	Quan.	Price ($)	Total ($)
Lens					
f=50 mm Achromatic Doublet	Thorlabs	AC254-050-A-ML	1	106.05	106.05
f=100 mm Achromatic Doublet	Thorlabs	AC254-100-A-ML	1	106.05	106.05
f=150 mm Achromatic Doublet	Thorlabs	AC254-150-A-ML	3	106.05	318.15
Optomechanics					
30 mm Cage Cube with Dichroic Filter Mount	Thorlabs	CM1-DCH	1	175.31	175.31
Kinematic Prism Mount	Thorlabs	KM100PM	1	80.07	80.07
Mounted Standard Iris	Thorlabs	ID25	1	60.87	60.87
Precision Optical Rail	Newport	PRL-6	1	165	165
Rail Carrier PRL Series	Newport	PRC-3	1	107	107
Filters, Dichroics and Wheel					
Laser polychroic mirror	Chroma	zt405/488/561/647/752rpc-UF2	1	975	975
Emission Filter ET445/58m	Chroma	ET445/58m	1	325	325
Emission Filter ET525/50m	Chroma	ET525/50m	1	325	325
Emission Filter ET605/70m	Chroma	ET605/70m	1	325	325
Emission Filter ET700/75	Chroma	ET700/75	1	325	325
Emission Filter ET800/60	Chroma	ET800/60	1	325	325
Motorized Filter Wheels	Thorlabs	FW102C	1	1211.97	1211.97
Mirrors					
Broadband Dielectric Mirror	Thorlabs	BB1-E02	5	77.35	386.75
Beam Shaper					
Topag top hat beam shaper, 250mm WD 4x4mm top hat 400-700nm AR/AR	CourierTronics	GTH-5-25-4	1	668	668
Topag positioner for GTH-5-25-4	CourierTronics	HSF01	1	176	176
Photomask for Spinning Disk					
5X5X.090 Quartz ND5 10um Resolution, cut and center hole, both sides BBAR	Front Range Photomask	NA	1	974	974
Fasteners and Miscellaneous					
Screw 2-56 Thread Size, 3/8"	McMaster	91253A079	1	6.09	6.09
O-Ring Dash Number 016	McMaster	9452K6	1	4.46	4.46
O-Ring Dash Number 022	McMaster	9452K76	1	5.93	5.93
Yeeco 5-12V BLDC motor controller	Amazon	B07BQYYDPH	1	12.99	12.99
				Grand Total	**7164.69**

Alternative or Optional Components

5x5x.090 LRC Chrome 10um Resolution Mask, cut and center hole	Front Range Photomask	NA	1	392	392
Laser polychroic mirror	Chroma	ZT405/488/561/647 rpc	1	550	550
Bandpass Emission Filter	Chroma	ET605/70m-2p	1	475	475
Bandpass Emission Filter	Chroma	ET525/50m-2p	1	475	475
Externally SM1-Threaded End Cap	Thorlabs	SM1PL	2	15.48	30.96
Externally SM1-Threaded Plug	Thorlabs	SM1CP2	2	18.83	37.66

Table S2. Summary of sample preparation and imaging conditions.

Figure	Specimen	**1° Ab** (1-2 µg/mL) **or FISH**	**2° Ab** (2-5 µg/mL or as indicated) **or FISH**	**Additional Stains**	**Imaging Cocktail**	**Objective lens**	**Disk Sector**	**Illumination & Area**	**Intensity at sample, exposures, Z-step size**
3 a-d	Beads (fluoresbrite YG 0.1 µm)					100× 1.45 NA oil (n = 1.512)	3	2× expand 80×80 µm^2	488 nm: 18 W/cm^2 133 ms exposures
3 f-g	1M fluorescein solution					100× 1.45 NA oil (n = 1.512)	prototype disk *d* = 50 µm *s* = 250 µm or *s* = 500 µm		
4 a-f	BS-C-1 cells, extracted then PFA/GA fixed	Rat x tTub Rb x dTub Ms x Vim	D x Rat AF750 (3.5 d/p) D x Rb AF568 (7.5 d/p) D x Ms AT488 (6 d/p)	Phalloidin AF647 0.6 µM, Hoechst 2 µg/mL in PBS	Glox + 1 mM trolox	60× 1.27 NA water	3	2× expand 130×130 µm^2	405: 2 W/cm^2 488: 7 W/cm^2 561: 6 W/cm^2 647: 4 W/cm^2 750: 7 W/cm^2 266 ms exposures 250 nm z-steps
4 g-i	RPE-1 cells, PFA fixed	GAPDH probe set, 150 nM, overnight 37 °C	Sequence P5 AT565 reporter oligo, 20 nM in 2× SSC	TO-PRO-3 1 µM	0.02× SSC (3× expansion)	60× 1.27 NA water	5	2× expand 130×130 µm^2	561: 32 W/cm2 647: 2 W/cm2 266 ms exposures 250 nm z-steps
4 j-k	Perfusion PFA fixed mouse brain, 100 µm slice	Rb x Homer Ms x Bassoon Rat x mCherry	D x Rb AF488 (8.5 d/p) D x Ms AT647N (3.5 d/p) D x Rat AT565 (3.8 d/p)		water (4× expansion)	60× 1.27 NA water	5	2× expand 130×130 µm^2	488: 5 W/cm^2 561: 10 W/cm^2 647: 7 W/cm^2 266 ms exposures 500 nm-z steps
5 a-c	RPE-1 cells, extracted then PFA/GA fixed	Rat x Tub	D x Rat Biotin (2 µg/mL) D x Rat AT488 (7 d/p, 0.2 µg/mL)	streptavidin 5 µg/mL, then sequence P1C biotin 500 nM	PAINT imaging buffer Sequence P1 Cy3B 0.05 nM	100× 1.45 NA oil	2	None 40×40 µm^2	488: 10 W/cm^2 561: 135 W/cm^2 106 ms exposures
5 f-g	B-SC-1 cells, extracted, then PFA/GA fixed	Rat x Tub	D x Rat AF647 (4.6 d/p)		Glox + 143 mM βME	100× 1.45 NA oil	prototype disk *d* = 70 µm *s* = 350 µm	2× contract 20×20 µm^2	647: 1 kW/cm^2 66 ms exposures
5 h,i	PtK-1 cells, extracted, then PFA/GA fixed	Rat x Tub Ms x Tub	D x Rat AF647 (4.6 d/p) D x Ms AF647 (5.3 d/p)		Glox + 143 mM βME	100× 1.45 NA oil	2	2× contract 20×20 µm^2	647: 1.2 kW/cm^2 26 ms exposures
S3, Table 2	Beads (Tetraspeck 0.1 µm or 0.2 µm)				Optical cement Water Air Air	100× 1.45 NA oil 60× 1.27 NA water 100× 0.9 NA air 20× 0.45 NA air	Various sectors	2× expand 80×80 µm^2	all: ~20 W/cm^2 266 ms exposures
S4, Table 2	BS-C-1 cells, extracted, then PFA/GA fixed	Rat x Tub	D x Rat AF405 (2 d/p) D x Rat AT488 (7 d/p) D x Rat AF568 (3.4 d/p) D x Rat AF647 (4.6 d/p) D x Rat AF750 (3.5 d/p)		Glox + 1 mM trolox or Glox + 1 mM trolox + 60% sucrose for oil imaging	100× 1.45 NA oil 60x 1.27 NA water 100x 0.9 NA air 20x 0.45 NA air	Various sectors	2× expand 80×80 µm^2 or 130×130 µm^2	all: ~10 W/cm^2 266 ms exposures

Abbreviations: 1° Ab = primary antibody; 2° Ab = secondary antibody; AF = Alexa Fluor; AT = ATTO-TEC; *d* = disk pinhole diameter; d/p = average number of dye molecules per protein; D x Rat = donkey anti-rat IgG; D x Rb = donkey anti-rabbit IgG; D x Ms = donkey anti-mouse IgG; GA = glutaraldehyde; Glox = glucose oxidase and catalase mixture; NA = numerical aperture; PBS = phosphate buffered saline; PFA = paraformaldehyde; *s* = inter-spiral spacing; SSC = saline sodium citrate; tTub = tyrosinated tubulin; dTub = detyrosinated tubulin; Vim = vimentin.

Notes: Illumination intensities are reported as average intensity across the field of view.

Table S3. DNA sequences for GAPDH mRNA FISH and DNA PAINT.

GAPDH Probes	Sequence
GAPDH_P01	GGGTGGAATCATATTGGAACATGTAAACCATGTTAATGATACGGCGACCACCGA
GAPDH_P02	AGCCAAATTCGTTGTCATACCAGGAAATGAGCTTAATGATACGGCGACCACCGA
GAPDH_P03	TGGTGATGGGATTTCCATTGATGACAAGCTTCTTAATGATACGGCGACCACCGA
GAPDH_P04	TTTACCAGAGTTAAAAGCAGCCCTGGTGACTTAATGATACGGCGACCACCGA
GAPDH_P05	TTTATTGATGGTACATGACAAGGTGCGGCTCCTTAATGATACGGCGACCACCGA
GAPDH_P06	CAAAAGAAGATGCGGCTGACTGTCGAATTAATGATACGGCGACCACCGA
GAPDH_P07	TTCAAGGGGTCTACATGGCAACTGTGATTAATGATACGGCGACCACCGA
GAPDH_P08	TTCTCATGGTTCACACCCATGACGAACATGGTTAATGATACGGCGACCACCGA
GAPDH_P09	GGCATTGCTGATGATCTTGAGGCTGTTGTCTTAATGATACGGCGACCACCGA
GAPDH_P10	ACGCCTGCTTCACCACCTTCTTGATGTCATCATTAATGATACGGCGACCACCGA
GAPDH_P11	TCTCAGCCTTGACGGTGCCATGGAATTTGTTAATGATACGGCGACCACCGA
GAPDH_P12	ACTTGATTTTGGAGGGATCTCGCTCCTGGTTAATGATACGGCGACCACCGA
GAPDH_P13	GGACTGTGGTCATGAGTCCTTCCACGATATTAATGATACGGCGACCACCGA
GAPDH_P14	CAAAGTGGTCGTTGAGGGCAATGCCATTAATGATACGGCGACCACCGA
GAPDH_P15	AGTTGTCATGGATGACCTTGGCCAGGTTAATGATACGGCGACCACCGA
GAPDH_P16	CAGTAGAGGCAGGGATGATGTTCTGGTTAATGATACGGCGACCACCGA
GAPDH_P17	TCGCTGTTGAAGTCAGAGGAGACCACTTAATGATACGGCGACCACCGA
GAPDH_P18	GACCAAATCCGTTGACTCCGACCTTCACCTTAATGATACGGCGACCACCGA
GAPDH_P19	TTCTCCATGGTGGTGAAGACGCCAGTGTTAATGATACGGCGACCACCGA
GAPDH_P20	GTCTTACTCCTTGGAGGCCATGTGGGTTAATGATACGGCGACCACCGA
GAPDH_P21	CCACAGTCTTCTGGGTGGCAGTGATGTTAATGATACGGCGACCACCGA
GAPDH_P22	GTTCAGCTCAGGGATGACCTTGCCCATTAATGATACGGCGACCACCGA
GAPDH_P23	CAGGTCAGGTCCACCACTGACACGTTTTAATGATACGGCGACCACCGA
GAPDH_P24	CTCAGTGTAGCCCAGGATGCCCTTGATTAATGATACGGCGACCACCGA
GAPDH Reporter	ATTO565-CTGTAGCAGTTCGGTGGTCGCCGTATCATT
DNA PAINT	
P1C (docking)	Biotin-TTTTTATACATCTA
P1 (imaging)	CTAGATGTAT-Cy3B

Table S4. Summary of Point Spread Functions for different disk and objective combinations.

Pinhole Dia (µm)	λ_{ex}	X-FWHM (µm)	stdX-FWHM	Z-FWHM (µm)	stdZ-FWHM	Sample
20× 0.45 NA Air						
35	488	0.80	0.06	4.89	0.19	TS200
35	561	0.84	0.05	4.95	0.11	"
35	647	0.85	0.03	5.38	0.07	"
50	488	0.75	0.03	4.72	0.20	"
50	561	0.80	0.02	5.32	0.21	"
50	647	0.88	0.01	6.23	0.17	"
100× 0.9 NA Air						
35	488	0.298	0.008	0.69	0.01	TS100
35	561	0.325	0.009	0.78	0.02	"
35	647	0.370	0.008	0.89	0.04	"
50	488	0.317	0.010	0.74	0.01	"
50	561	0.334	0.007	0.81	0.01	"
50	647	0.386	0.008	0.93	0.02	"
60× 1.27 NA Water						
35	488	0.32	0.01	0.77	0.04	TS100
35	561	0.34	0.02	0.74	0.03	"
35	647	0.337	0.008	0.72	0.01	"
50	405	0.30	0.05	1.37	0.08	"
50	488	0.308	0.008	0.82	0.04	"
50	561	0.33	0.01	0.83	0.04	"
50	647	0.353	0.005	0.85	0.02	"
50	750	0.44	0.03	1.04	0.05	"
100× 1.45 NA Oil						
20*	488	0.24	0.02	0.40	0.01	TS100
20*	561	0.25	0.02	0.40	0.02	"
20*	647	0.25	0.02	0.47	0.04	"
30*	488	0.22	0.01	0.42	0.01	"
30*	561	0.23	0.01	0.41	0.01	"
30*	647	0.250	0.008	0.48	0.02	"
35	488	0.207	0.005	0.42	0.01	"
35	561	0.225	0.005	0.42	0.01	"
35	647	0.270	0.006	0.49	0.02	"
40*	488	0.224	0.007	0.45	0.01	"
40*	561	0.236	0.009	0.45	0.01	"
40*	647	0.260	0.007	0.51	0.02	"
50	405	0.22	0.01	0.96	0.16	MT
50	488	0.222	0.004	0.49	0.02	TS100
50	561	0.237	0.003	0.50	0.02	"
50	647	0.273	0.003	0.56	0.02	"
50	750	0.35	0.02	0.61	0.03	MT
70*	488	0.229	0.001	0.51	0.01	"
70*	561	0.244	0.005	0.52	0.01	"
70*	647	0.276	0.004	0.60	0.01	"

Notes:

1) X-FWHM and stdX-FWHM refer to the average lateral full-width at half maximum from Gaussian fits and the standard deviation from many such fits. Z-FWHM and stdZ-FWHM refer to the average axial full-width at half maximum from Gaussian fits and the standard deviation from many such fits.

2) Point spread function widths were determined from either 100 nm Tetraspeck beads (TS100), 200 nm Tetraspeck beads (TS200), or microtubule samples (MT).

3) * denotes a disk without an anti-reflection coating.

4) The inter-spiral spacing for all sectors was equal to 5x the pinhole diameter.

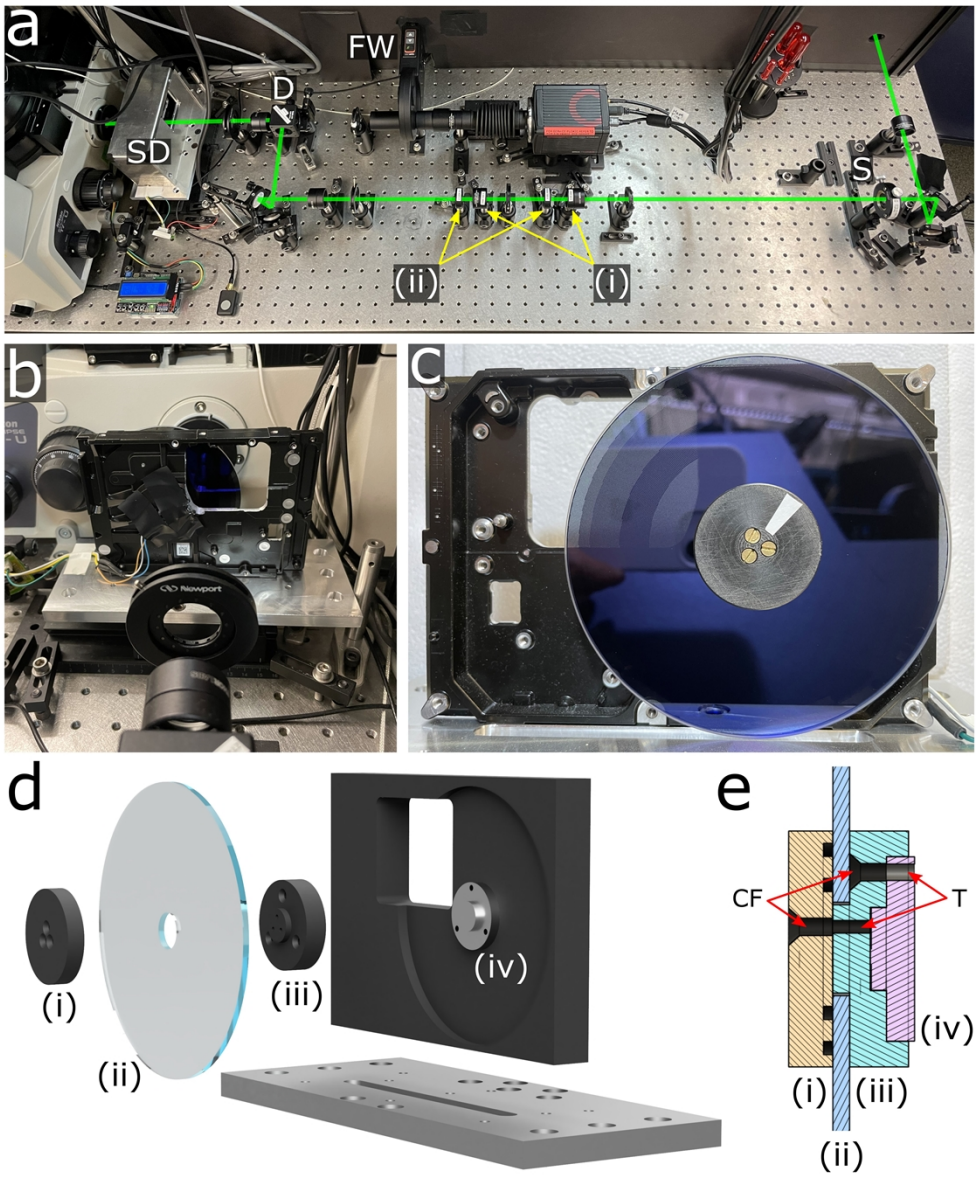

Figure S1. *DIY SDCM setup and schematic diagrams. (a) Photograph of DIY SDCM with selected components highlighted: Spinning disk (SD) in its protective housing, dichroic (D), filter wheel (FW) and square shaper (S). The excitation laser path is highlighted in green, with 2× expanding telescope lenses (i) for general illumination, or 2× demagnifying telescope lenses for high power density (STORM illumination) by reversing the lens order in the marked optical mounts (ii). Alternatively, the telescope lenses can be omitted and the shaper repositioned for no magnification (DNA-PAINT illumination). (b) Photograph of spinning disk with housing removed. The commercial hard drive motor-base assembly is modified to include a machined window for the light path. (c) Photograph of the spinning disk showing the Delrin adapter and white tape mark used to trigger the tachometer circuit. (d) Schematic diagram and (e) cross-sectional view of spinning disk components and assembly. Marked components in (d) and (e) include (i) Delrin clamping plate, (ii) glass photomask, (iii) Delrin motor adapter, and (iv) hard drive spindle motor. Clearance and threaded holes are denoted CF and T, respectively. Note the O-ring grooves in the clamping plate ensure a strong grasp on the glass disk (see* ***Table S1*** *for part numbers). Refer to Code 3 for CAD files.*[1]

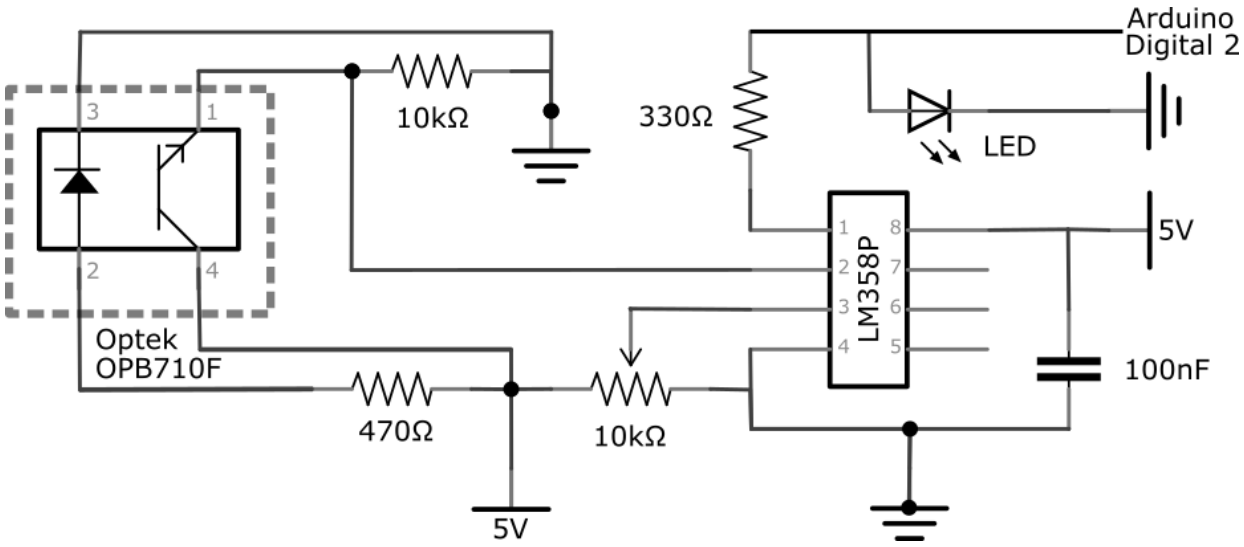

Figure S2. *Circuit schematic of spinning disk tachometer. A reflective phototransistor photodiode pair (Optek, OPB710F, 910 nm) was fitted into the spinning disk housing above the Delrin clamping plate, and a small strip of absorptive tape placed applied to provide a reflective signal difference. The detection threshold of the operational amplifier (LM358P) was adjusted using the potentiometer, and a LED provided a visual readout. The digital output signal of the circuit was wired to a microcontroller (Arduino Uno) which counted the pulses in a predetermined time window, and the rotation rate was displayed on an LCD shield (DFRobot, DFR0009). The reflective sensor (dashed box) was connected on long flexible wires for ease of placement. Practically, we found it was unnecessary to trigger the camera from the disk rotation signal, instead setting an exposure time approximately equal to an integer number of disk rotations was sufficient to avoid any streaking artifacts. Refer to Code 4 for corresponding Arduino code.*[2]

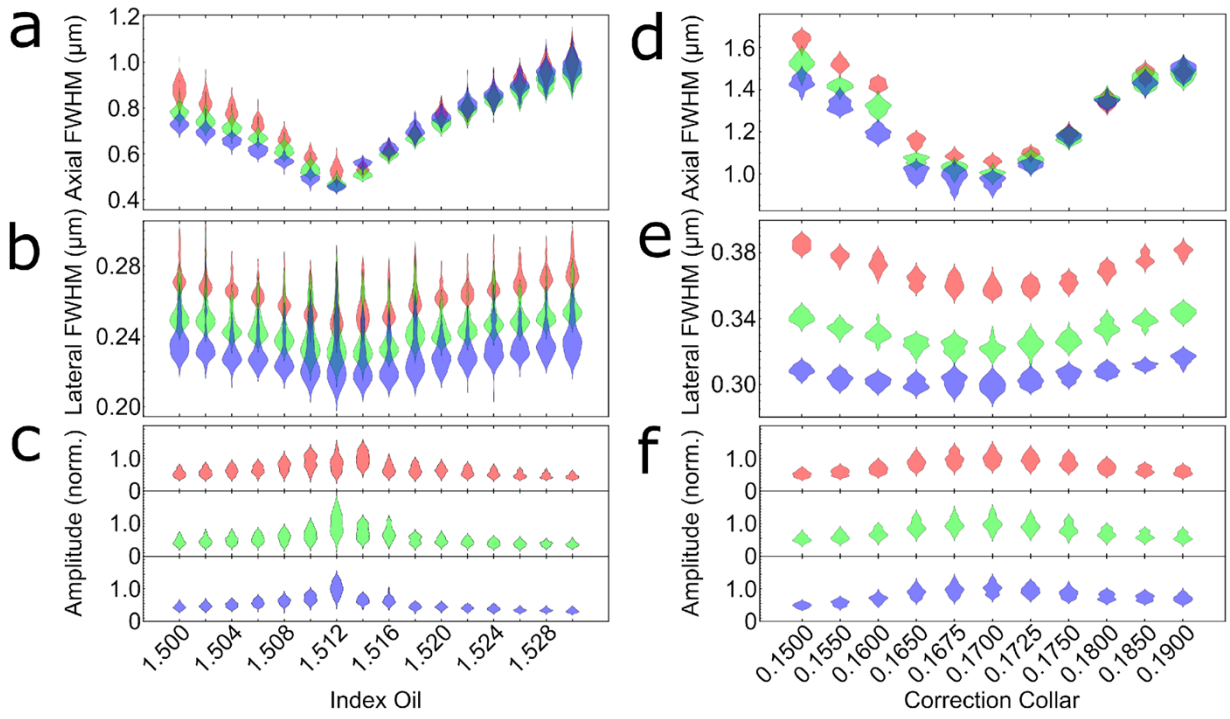

Figure S3. *PSF axial FWHM, lateral FWHM, and maximum amplitude by varying index matching oil of a 100× 1.45NA oil immersion objective (a-c), or by varying the correction collar of a 60× 1.27NA water immersion objective (d-f), respectively. The analysis was performed on 100 nm Tetraspeck beads excited at 488 nm (blue), 561 nm (green) and 647 nm (red) using d = 50 µm and s = 250 µm. For the oil lens (a-c), the beads were adsorbed to a coverglass and embedded in optical cement (Nordland NOA60), and >90 beads were analyzed for each index oil. For the water lens (d-f), the beads were adsorbed to a coverglass, covered with water, and >60 beads were imaged for each collar position.*

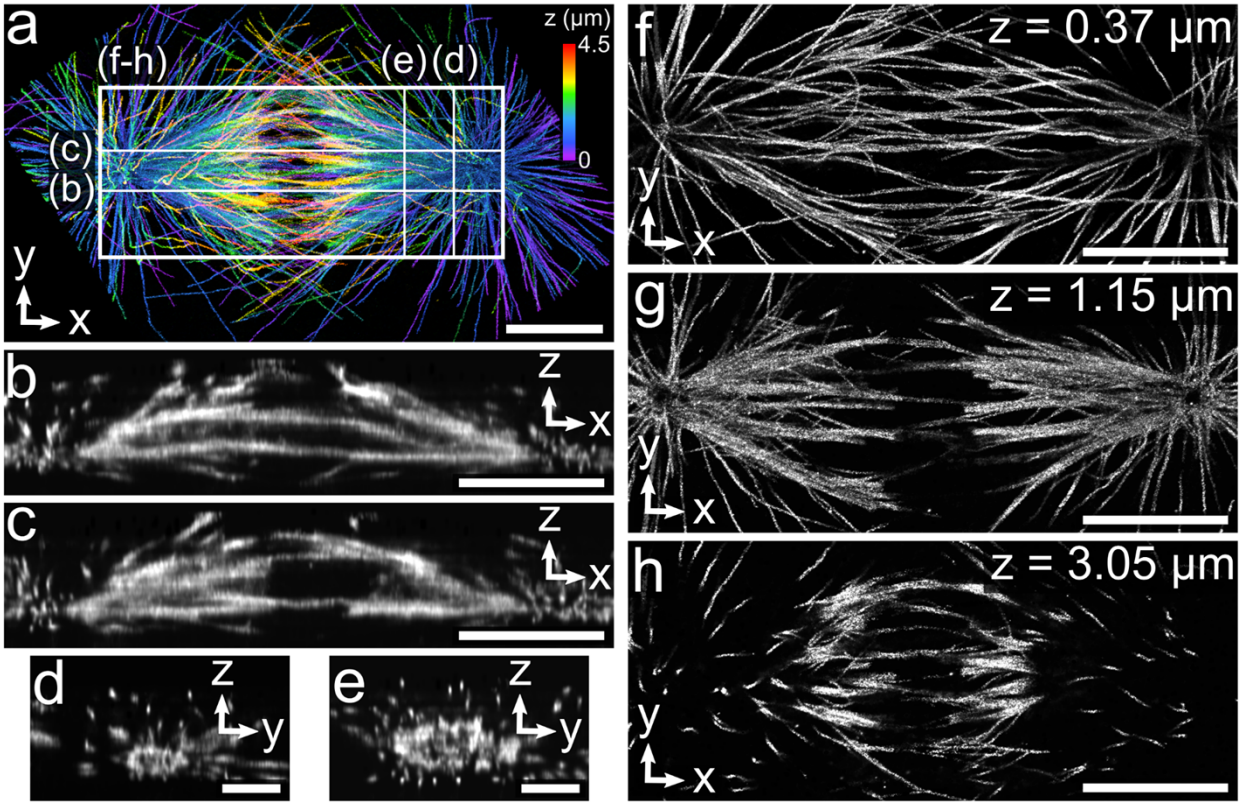

Figure S4. *Single-molecule localization microscopy of a dividing PTK-1 cell using SDC microscope. (a) Maximum intensity projection of 3D STORM image of immunostained microtubules from a 4.5 μm thick dividing PTK-1 cell with z-dimension position colorized according to the color scale bar. (b-e) Cross-section corresponding to the planes denoted in* ***a****. (f) Maximum intensity projection of a 0.75 μm thick image centered at z=0.37 μm and (g,h) 50 nm thick z-sections corresponding to the z-height denoted in the figure for the area highlighted in* ***a****. Scale bars 5 μm (a-c, f-h), 2 μm (d,e).*

Supplemental Note 1: Alignment

The alignment process is analogous to that of an epifluorescence microscope for most steps, however, in this design, the dichroic is placed external to the microscope chassis, and an empty cube is used in microscope turret. Once the microscope is set up for epifluorescence imaging in this way, two unique steps to the SDCM are described as follows. First, the spinning disk pinholes must be carefully placed at the image plane of the microscope. The positions of L_4, L_5 and the camera can be set without the disk in the emission path. Next, the disk is inserted near the image plane using white light illumination provided by the microscope condenser. The position of the disk at the image plane is set by carefully sliding it along the optical axis until the stationary pinholes are in sharp focus on the camera to determine the image plane. Observing the pinholes in sharp focus may be facilitated using larger pinholes (>50 μm) if available. Second, the iris between L_4 and L_5 can be stopped down to lower background, but not appreciably reduce fluorescence signal. In addition, the spinning disk can then be rotated slightly off perpendicular to the optical axis such that the reflected excitation beam is rejected by the iris. Of final note, we observed that it was best to face the reflective metal side of the spinning disk toward the camera to reduce any autofluorescence background generated by the disk substrate.

Supplemental Note 2: Spatial Resolution

According to Wilson [3], the lateral diffraction-limited resolution, $LFWHM_{confocal}$, of an idealized confocal microscope with an infinitesimally small pinhole and homogenous pupil illumination can be calculated using the equation below, where λ is the wavelength of light (assuming a small Stokes shift), and *NA* is numerical aperture of the objective lens.

$$LFWHM_{confocal} = \frac{0.37\lambda}{NA}$$

For a very large pinhole, which corresponds to that of a widefield microscope, Wilson [3] also provides.

$$LFWHM_{wide} = \frac{0.51\lambda}{NA}$$

Wilson [3] and Amos [4] provide equations for calculation of the axial diffraction-limited spatial resolution for an idealized confocal microscope with an infinitesimal pinhole and very large (widefield) pinholes

$$Z_{FWHM\ confocal} = \frac{0.64\lambda}{n - \sqrt{n^2 - NA^2}}$$

$$Z_{FWHM\ wide} = \frac{0.89\lambda}{n - \sqrt{n^2 - NA^2}}$$

In the case of a finite-sized pinhole, the theoretical lateral and axial diffraction-limited spatial resolution would fall between the respective confocal and widefield diffraction-limited resolutions shown above.

We used a numerical procedure described by Amos [4] and by Sandison [5] that incorporates the pinhole size when calculating theoretical diffraction-limited lateral and axial resolution for a point source, and we show in **Table S5**, below, these theoretical values in comparison with our measured FWHM values. One would expect to see a higher spatial resolution for shorter wavelengths, higher numerical aperture, and higher-index immersion medium; higher spatial resolution is also expected for a smaller pinhole, although this comes with the tradeoff of a significantly reduced signal at very small pinhole values. Although all of our measured resolution values are larger than the theoretical values, we can indeed see that the expected trends are generally observed. It should be noted that the theoretical equations listed above are in the absence of spherical aberration, such as those caused by refractive index mismatch between the immersion medium and the coverglass, that can degrade axial resolution.[6,7] Partial aberration compensation can be accomplished using the methods demonstrated in Supplemental Figure 3.

Table S5. Comparison of Measured Spatial Resolution and (Predicted) Diffraction-Limited Resolution.

				Measured		**Diffraction-Limited**	
λ	***NA***	***D***	***n***	**LFWHM**	**AFWHM**	**LFWHM**	**AFWHM**
405 nm	1.45	50	1.512	220 nm	960 nm	143 nm	296 nm
488 nm	1.45	50	1.512	222 nm	490 nm	173 nm	335 nm
561 nm	1.45	50	1.512	237 nm	500 nm	197 nm	363 nm
647 nm	1.45	50	1.512	273 nm	560 nm	221 nm	398 nm
750 nm	1.45	50	1.512	350 nm	610 nm	245 nm	445 nm
488 nm	1.27	35	1.33	320 nm	770 nm	197 nm	403 nm
561 nm	1.27	35	1.33	340 nm	740 nm	226 nm	437 nm
647 nm	1.27	35	1.33	337 nm	720 nm	262 nm	478 nm
488 nm	1.45	20	1.512	240 nm	400 nm	139 nm	280 nm
488 nm	1.45	30	1.512	220 nm	420 nm	155 nm	287 nm
488 nm	1.45	40	1.512	224 nm	450 nm	169 nm	306 nm

Abbreviations: *NA* = numerical aperture; *D* = pinhole diameter; *n* = index of refraction; LFWHM is lateral full-width at half maximum; AFWHM is axial full-width at half maximum.

Supplemental Note 3: Requirements for Base System

The design for the spinning disk confocal module we presented should be compatible with a range of conventional microscopes. Minimum requirements for the conventional microscope include the following.

- A suitable objective lens (e.g., 100× 1.45 NA oil immersion, 60× 1.27 NA water immersion, or 20× 0.45 NA air lens, as described in Table 1).
- A port for accessing the microscope light path, such as the right-port on our Nikon Ti-U microscope shown in Figure S1. Commercial microscope stands from most major manufacturers include these, including those from Leica, Olympus, Zeiss, as well as other chassis from Nikon.
- There should be a means to axially scan the sample focal plane (e.g., a piezo positioner) and there should be a motorized or manual stage to enable lateral positioning of the sample.
- A camera will be required. Our Hamamatsu Orca v3 sCMOS camera has 6.5 μm square pixels; cameras with pixels of a different size may require a different magnification of the image in the detection path.

A major tradeoff of our simple and inexpensive microlens-free spinning disk confocal microscope design is that the efficiency of excitation light transmitted by the pinhole array is relatively low. For example, as shown in Table 1, disk sector 3 has 50 μm diameter pinholes and a 250 μm spacing, yielding a fill factor of 0.031, or approximately 3.1% transmission of excitation light through the pinhole array. In comparison, commercial microlens spinning disk systems often have transmissions that exceed 50%. This ~16-fold loss in excitation transmission can be compensated by using high-power lasers or by adjusting illumination area or exposure duration. The relatively high-power lasers we used are convenient (at the laser heads, the systems put out maximum powers of 200 mW at 405 nm, 1 W at 488 nm, 2 W at 561 nm, 1.5 W at 647 nm, and 500 mW at 750 nm) but we often used laser powers at the disk in the range 20-200 mW for 266 ms exposures and ~1000 × 1000 pixels areas. We discuss adjustment of the illuminated area in Section 3.4.2, Figure 1a-c, and Figure S1a.

References

1. A. R. Halpern, M. Y. Lee, M. D. Howard, M. A. Woodward, P. R. Nicovich, and J. C. Vaughan, "Versatile, do-it-yourself, low-cost spinning disk confocal microscope Code 3," https://osapublishing.figshare.com/s/c5bc145bbb35b4113c93.
2. A. R. Halpern, M. Y. Lee, M. D. Howard, M. A. Woodward, P. R. Nicovich, and J. C. Vaughan, "Versatile, do-it-yourself, low-cost spinning disk confocal microscope Code 4," https://osapublishing.figshare.com/s/69563957fe9cb3dfe9b3.
3. T. Wilson, "Resolution and optical sectioning in the confocal microscope," Journal of Microscopy **244**(2), 113–121 (2011).
4. B. Amos, G. McConnell, and T. Wilson, "Confocal Microscopy," in *Comprehensive Biophysics*, 1st ed. (Elsevier, 2012).
5. D. R. Sandison, D. W. Piston, R. M. Williams, and W. W. Webb, "Quantitative comparison of background rejection, signal-to-noise ratio, and resolution in confocal and full-field laser scanning microscopes," Appl. Opt. **34**(19), 3576 (1995).
6. C. J. R. Sheppard, M. Gu, K. Brain, and H. Zhou, "Influence of spherical aberration on axial imaging of confocal reflection microscopy," Appl. Opt. **33**(4), 616 (1994).
7. S. Hell, G. Reiner, C. Cremer, and E. H. K. Stelzer, "Aberrations in confocal fluorescence microscopy induced by mismatches in refractive index," Journal of Microscopy **169**(3), 391–405 (1993).